Chemico-Biological Interactions 284 (2018) 56–68

Contents lists available at ScienceDirect

Chemico-Biological Interactions

journal homepage: www.elsevier.com/locate/chembioint

Renal toxicological evaluations of sulphonated nanocellulose from *Khaya sengalensis* seed in Wistar rats

Adewale Adewuyi[a,b,*], Chiagoziem A. Otuechere[a], Olusegun L. Adebayo[a], Chibuzo Anazodo[a], Fabiano V. Pereira[b]

[a] Department of Chemical Sciences, Faculty of Natural Sciences, Redeemer's University, Ede, Osun state, Nigeria
[b] Department of Chemistry, Federal University of Minas Gerais, Av. Antônio Carlos, 6627, Pampulha, CEP 31270-901, Belo Horizonte, MG, Brazil

ARTICLE INFO

Keywords:
Inflammation
Khaya sengalensis
Kidney
Nanocellulose
Toxicity

ABSTRACT

Nanocellulose is currently gaining attention due to its unique properties. This attention includes its application as building blocks for developing novel functional materials, plant drug and also in drug delivery systems. However, its safety remains largely untested or less understood. Thus, sulphonated nanocellulose (KSS) was prepared from cellulose (KSC) isolated from *Khaya senegalensis* seed (KS). KS, KSC and KSS were characterized using Fourier transformed infrared (FTIR), X-ray diffraction (XRD), thermogravimetric analysis (TG), particle size distribution (PSD), zeta potential and scanning electron microscopy (SEM). The impact of KSS on selected renal markers of oxidative stress, inflammation and apoptosis in Wistar rats was also investigated. Thus, male rats were randomly assigned to four groups of five animals each and were treated with KSS (0, 50, 75 and 100 mg/kg BW) for 14 days. Thereafter, biomarkers of renal oxidative damage, inflammation and immunohistochemical expressions of iNOS, COX-2, Bcl-2 and p53 were evaluated. The results revealed KSS to have crystallinity of 70.40%, it was monomodal and has a flaky surface with agglomerations. KSS had no effect on markers of kidney function and oxidative damage, although there was a generalized hypernatremia after 14 days of exposure. Lastly, KSS enhanced the antioxidant status and immunohistochemical expressions of iNOS and COX-2 in the kidney of the rats. While the biomedical applications of KSS may appear plausible, our data suggests that it could induce renal toxicity via the combined impacts of electrolyte imbalance and inflammation.

1. Introduction

The use of plant sourced materials as drug plays a major role in the management of kidney diseases [1]. This is mostly reflected in the case of people living in developing countries where traditional medicine has become paramount in primary health care [2]. A few of these plant sourced materials have been reported to possess nephroprotective and anti-inflammatory activities [3]. This they do mostly by improving antioxidant status which is preventive and passive for defending against damages [4]. Although several plant sourced materials have been reported but some of them have short comings such as dosage effectiveness, toxicity, purity, lack of efficacy and side effect [5]. This has led to different treatment options for common kidney diseases, a few of these therapy are modern but some of them still lack efficacy while a few others are with side effects since most of them are from synthetic petrochemicals with risk of adverse effects [6]. So, there is need for effective therapeutic agents which is from a renewable source, environmentally friendly, cost effective and with a low or no side effect.

Most chronic renal diseases such as diabetic nephropathy and chronic glomerulonephritis will most times result to renal fibrosis which is characterized by tissue damage leading to excessive inflammation [7]. This has shown that treatment of chronic renal diseases needs to target acute and chronic inflammation, as well as progressive renal fibrosis. Some treatments have been recorded in the past but some of them suffer from some limitations which have led to search for new approaches. One of the considered approaches is the use of nanomaterial as protective agents [8]. Some of these nanomaterials have also shown potential application in disease control but a number of them need to be evaluated for their toxicity levels.

Nanocellulose is an example of nanomaterials that is being used as building blocks for development of novel functional materials and recently it has been gaining application in plant drug and drug delivery system [9]. Modification of nanocellulose with the introduction of different functionality has played important role in improving on its properties for its several applications [10]. Surface modification of nanocellulose has contributed significantly to improving its capacity as

* Corresponding author. Department of Chemical Sciences, Faculty of Natural Sciences, Redeemer's University, Ede, Osun state, Nigeria.
E-mail address: adewuyia@run.edu.ng (A. Adewuyi).

https://doi.org/10.1016/j.cbi.2018.02.015
Received 21 September 2017; Received in revised form 19 January 2018; Accepted 13 February 2018
Available online 16 February 2018
0009-2797/ © 2018 Elsevier B.V. All rights reserved.

plant drug agents but its toxicity still remains questionable as this required proper investigation [11]. Previously reported toxicological evaluations of nanocellulose materials have focused primarily on the unmodified nanocellulose materials with regards to cytological or inhalation toxicity, but there is rare or very limited data on animal model toxicity study with respect to the impact of surface modifications [12,13]. Some of the previously reported modifications include; succination, silylation, acetylation, amidation, grafting and carboxylation [14–16]. Although most surface modifications processes are benign [17] but there is still need to evaluate them for potential toxicity. These modifications rely on the hydroxyl functional groups on the surface of nanocellulose [17]. Despite several improvements attained from these modifications, there are still limited data regarding the toxicity potentials of most of these modified nanomaterials [13].

Since the ability of nanocellulose to function as plant drug and in drug delivery system is based on its surface chemistry, it is eminent to consider the effect of its surface chemistry on biological systems. So, studying the interaction between biological system and surface modified nanocellulose is one of the keys to understanding its toxicity and safety profile. Thus, this study has evaluated the possible toxicity of KSS on the kidney of Wistar rats. There is no need to check the toxicity of KSC since cellulose has been identified to be safe by Food and Drug Administration [18] but the safety of nanocellulose and its modified forms remains a question to be solved.

In response to this quest, KSS was prepared from KSC isolated from underutilized *Khaya senegalensis* seed. This was achieved via simple chemical reaction route. The impact of KSS on selected renal markers of oxidative stress, inflammation and apoptosis in Wistar rats fed with KSS for 14 day was investigated. Biomarkers of renal oxidative damage, inflammation and immunohistochemical expressions of iNOS, COX-2, Bcl-2 and p53 were also evaluated.

2. Materials and methods

2.1. Materials

KS was obtained from a garden in Ibadan, Oyo state, Nigeria. This was later identified at the Department of Botany and Microbiology, University of Ibadan, Ibadan, Oyo state, Nigeria. KS was ground in an industrial mill and deffated by subjecting it to soxhlet extraction using n-hexane as previously described by Adewuyi et al. [19]. This was later air dried and stored in an airtight container. Sodium chlorite, sodium hydroxide and acetic acid were purchased from Sigma-Adrich (Brazil) while sodium chloride, potassium chloride, epinephrine, 1-chloro-2, 4-di nitrobenzene (CDNB), 5′,5′- Dithiobis-2-nitrobenzoic acid (DTNB), reduced glutathione (GSH), thiobarbituric acid (TBA) were obtained from Sigma Chemical Company (USA). Rabbit monoclonal COX-2, iNOS, Bcl-2 and p53 antibodies were obtained from Abcam (UK). All other chemicals used were of analytical grade and were obtained from Sigma-Aldrich, St. Louis, USA.

2.2. Isolation of KSC

Cellulose was isolated from KS as previously described [20]. Briefly, 350 g of the deffated KS was weighed and transferred into a 5 L beaker. This was treated with alkali solution (2 wt% NaOH) at 80 °C for 5 h under continuous stirring using a Fisatom mechanical stirrer. It was filtered, washed with deionized water until free of alkali and oven dried at 50 °C. The treatment with alkali solution was repeated twice. The residue obtained was bleached at 80 °C for 5 h with a mixture of solution which was made up of equal volumes (1:1) of acetate buffer (27 g NaOH and 75 mL glacial acetic acid, diluted to 1 L of distilled water) and aqueous sodium chlorite (1.7 wt% $NaClO_2$ in distilled water). The resulting fibers were washed repeatedly in deionized water until the pH of the fibers became neutral. The bleaching step was repeated twice until the fiber became completely white and dried in an air-circulating oven at 50 °C for 24 h resulting in cellulose (KSC) yield of about 30%.

2.3. Synthesis of KSS

Sulphonated nanocellulose was obtained by acid hydrolysis with 65% sulphuric acid solution (v/v) at 50 °C. To achieve this, KSC to acid ratio was maintained as 1:10 (g/mL) under strong mechanical stirring for 45 min. After hydrolysis, the dispersion was diluted two fold in deionized water and the suspension washed three times using a centrifuge (Eppendorf, 5810R, Hamburg, Germany) to remove the spent acid. The suspension was then subjected to ultrasonication in a Cole Parmer sonicator (model CV334) for 15 min to disperse the nanocrystals and break any agglomerates formed. After this, the suspension was dialyzed in deionized water to remove salts. The resulting KSS was stored at 4 °C.

2.4. Characterization

The functional groups in KS, KSC and KSS were determined using FTIR (Perkin Elmer, spectrum RXI 83303). The samples were blended with KBr, pressed into pellets and analyzed in the range of 400–4500 cm^{-1}. Surface morphology was studied using SEM (JEOL JSM-6360LV, Japan). For the SEM analysis, powdered KS, KSC and KSS were coated with gold using the sputtering technique in order to increase electrical conductivity and the quality of the micrographs. The X-ray diffraction pattern was obtained using X-ray diffractometer (XRD-7000X-Ray diffractometer, Shimadzu) with filtered Cu Kα radiation operated at 40 kV and 40 mA. The XRD pattern was recorded from 10 to 80° (2θ), with a scanning speed of 2°/min. Thermal stability and fraction of volatile components of KS, KSC and KSS were monitored by TGA. This was achieved using a simultaneous DTA-TG apparatus (SHIMADZU, C30574600245). KS, KSC and KSS was analyzed for their particle size distribution and zeta potentials using a zeta potential analyzer (DT1200, Dispersion technology) at 25 °C while observing general calculation model for irregular particles. This involved taking several measurements using Dispersion technology-AcoustoPhor Zeta size 1201 software (version 5.6.16).

2.5. Water holding capacity

Water holding capacity of KSS was determined as described by Zhang et al. [21]. This was evaluated by weighing 0.5 g (W_1) of KSS into 10 mL of distilled water in a pre-weighed, clean centrifuge tube (W) placed in a water bath at 37 °C for 30 min. The centrifuge tube and its content was centrifuged for 15 min at 4000 rpm; the supernatant was removed and the centrifuge tube with the distilled water soaked sample was weighed (W_2). Water holding capacity was estimated as:

$$WC\ (gg^{-1}) = \frac{(W_2 - (W + W_1)}{W_1} \quad (1)$$

2.6. Heavy metal adsorption capacity

Heavy metal adsorption capacity of KSS was determined using lead nitrate ($Pb(NO_3)_2$) and copper sulphate ($Cu(SO_4)\cdot 5H_2O$) salts solutions. Metal adsorption study was carried out by separately shaking 0.1 g of KSS with 50 mL solutions (100 mg/L) of metal in different beakers at 25 °C and 200 rpm for 3 h. This was later centrifuged for 10 min at 5000 rpm and the metal concentrations before and after adsorption were determined using Atomic Absorption Spectrometer (Varian AA240FS). The metal ions adsorption capacity of KSS was calculated using equation:

$$q_e = \frac{(C_o - C_e)V}{M} \quad (2)$$

Where q_e is the adsorption capacity in mg/g, C_o and C_e are initial and

final concentrations (mg/L) of adsorbate (Pb^{2+} and Cu^{2+}) in solution respectively; while V and M are volumes (L) of metal ions solution and weight (g) of KSS used.

2.7. Animals and treatment

The treatment was carried out using healthy sixteen male Wistar rats weighing approximately 160–190 g. The animals were obtained from the primate colony of the Department of Veterinary Pathology, University of Ibadan, Ibadan, Nigeria. Rats were fed on commercial pelleted diet (Ladokun Feeds, Ibadan, Nigeria) and drinking water ad libitum, maintained under standard laboratory conditions and subjected to natural photoperiod of 12 h light/12 h dark cycle. All animals received humane care in accordance with guidelines governing the handling of laboratory animals as outlined by the Redeemer's University Committee on Ethics for Scientific Research. The animals were housed in stainless cages with temperature maintained at 25 ± 2 °C.

Rats were randomly assigned to four groups of five animals each and were treated as follows for 14 days:

- Group A: Control animal fed with olive oil without KSS
- Group B: Fed with KSS (50 mg/kg body weight), orally, once, daily
- Group C: Fed with KSS (75 mg/kg body weight), orally, once, daily
- Group D: Fed with KSS (100 mg/kg body weight), orally, once, daily

These doses represent low, medium and high doses as previously reported for hydroxamic acid from *Cyperus esculentus* seed oil [22]. As the experiment proceeded, all animals were observed daily for clinical signs and symptoms of toxicity. At the end of the 14th day, the rats were sacrificed 24 h after the last treatment by cervical dislocation. The kidneys were harvested, washed free of extraneous materials and transferred into ice-cold 0.25 M sucrose solution, blotted with clean tissue paper and homogenized in phosphate buffer (0.1 M, pH 7.4). Homogenates were centrifuged at 10000 g for 20 min to obtain the post mitochondrial fraction. The supernatant was collected and used for the various biochemical measurements. A small section of the harvested organ was placed in phosphate buffer-formalin (PBF) for immunohistochemistry.

2.8. Estimation of renal somatic index

The kidneys were harvested and blot-dried using an absorbent filter paper. The whole body and organ weights in animals within the treatment groups were recorded using a sensitive weighing balance. The organosomatic index (OSI) was calculated using the following formula [23]:

$$OSI = \frac{Weight\ of\ organ\ (g)}{Body\ weight\ (g)}\ X\ 100 \quad (3)$$

2.9. Biochemical assays

2.9.1. Plasma clinical parameters

Biochemical analyses on biochemical markers were carried out to determine the plasma concentrations of Aspartate Amino Transferase (AST), albumin, uric acid and creatinine using diagnostic kits (Randox Laboratories Limited) as reported in previous studies [24]. The amount of potassium was determined by a precipitate techniques using sodium tetraphenyl boron as described by Wijesekera et al. [25]. The presence of sodium ion was determined as previously described [26] while a colorimetric procedure was used in order to estimate the calcium level as previously reported [25].

2.9.2. Superoxide Dismutase (SOD)

The activity of SOD in the organs of rats was determined using the method of Misra and Fridovich [27] based on the inhibition of autoxidation of epinephrine (pH 10.2) at 30 °C. The assay mixture contains 20 µL of the sample and 2.5 mL of 0.05 M carbonate buffer (pH 10.2). After equilibration in the spectrophotometer, freshly prepared solution of 0.3 mM epinephrine (0.3 mL) was added and mixed by inversion. Subsequently, the increase in absorbance at 480 nm was monitored in a spectrophotometer for 150 s at 30 s intervals. The activity of SOD was then expressed in Units/mg protein.

2.9.3. Catalase (CAT)

Catalase activity in tissue was assayed at room temperature following the procedure of Luck [28]. Briefly, 25 µL of sample was added to 3.0 mL of hydrogen peroxide-phosphate buffer (12.5 mM in 0.067 M sodium phosphate buffer, pH 7.0). Decomposition of hydrogen peroxide by catalase was measured at 240 nm for 3 min and the result was expressed as micromoles of H_2O_2 decomposed/min/mg protein. The molar extinction coefficient of H_2O_2 used was 71 $M^{-1}cm^{-1}$.

2.9.4. Glutathione peroxidase (GPx)

The activity of GPx was evaluated by the method of Rotruck et al. [29]. The reaction containing sodium phosphate buffer (500 µL), 10 mM of sodium azide (100 µL), 4 mM GSH (200 µL), 2.5 mM H_2O_2 (100 µL), and the sample (50 µL) was made up to 2 mL with distilled water. After incubation for 3 min at 37 °C, the reaction was terminated by the addition of 10% trichloroacetic acid (0.5 mL). The supernatant obtained after the centrifugation was used to determine the level of residual GSH by the addition of 4 mL of 0.3 M disodium hydrogen phosphate, and 1 mL of DTNB reagent. The absorbance was measured in a spectrophotometer at 412 nm and the GPx activity was expressed as Units/mg protein.

2.9.5. Glutathione-S-transferase (GST)

Glutathione-S-transferase (GST) activity was determined according to Habig et al. [30]. Briefly, the assay mixture containing 0.03 mL of sample, 2.79 mL phosphate buffer (0.1 M, pH 7.4), 0.15 mL of 1-chloro-2, 4,-dinitrobenzene and 0.03 mL of GSH (0.1 M) were mixed by inversion and immediately read at 340 nm against blank containing all the components except the enzyme source at 3 min at 60 s interval in a spectrophotometer. Activity was expressed as Units/mg protein.

2.9.6. Glutathione (GSH)

Analysis of GSH concentration was performed according to the method described by Beutler et al. [31]. In brief, 0.2 mL of tissue homogenates was added to 1.8 mL distilled water and 3.3 mL of 4% sulfosalicylic acid. The mixture was allowed to stand for approximately 5 min and filtered. To the supernatant, 0.5 mL of 5, 5′-dithiobis-(2-nitrobenzoic acid) (DTNB) was added in the presence of phosphate buffer (0.1 M, pH 7.4). The solution was kept at room temperature for 15 min and absorbance recorded at 412 nm was used for the estimation of GSH concentration.

2.9.7. Hydrogen peroxide

The levels of hydrogen peroxide generated in the kidney after exposure of rats to KSS was evaluated by the method of Wolff [32], based on ferrous oxidation with xylenol orange. The sample (50 µL) was added to a mixture of xylenol orange (100 µM), ammonium ferrous sulphate (250 mM), sorbitol (100 mM), and of H_2SO_4 (25 mM), and vortexed. After incubation at room temperature for 30 min, the absorbance was measured spectrophotometrically at 560 nm.

2.9.8. Malondialdehyde (MDA)

The MDA level was measured as thiobarbituric acid reactive substances in renal tissues according to the method described previously [33]. Briefly, an aliquot (0.4 mL) of the tissue post mitochondria

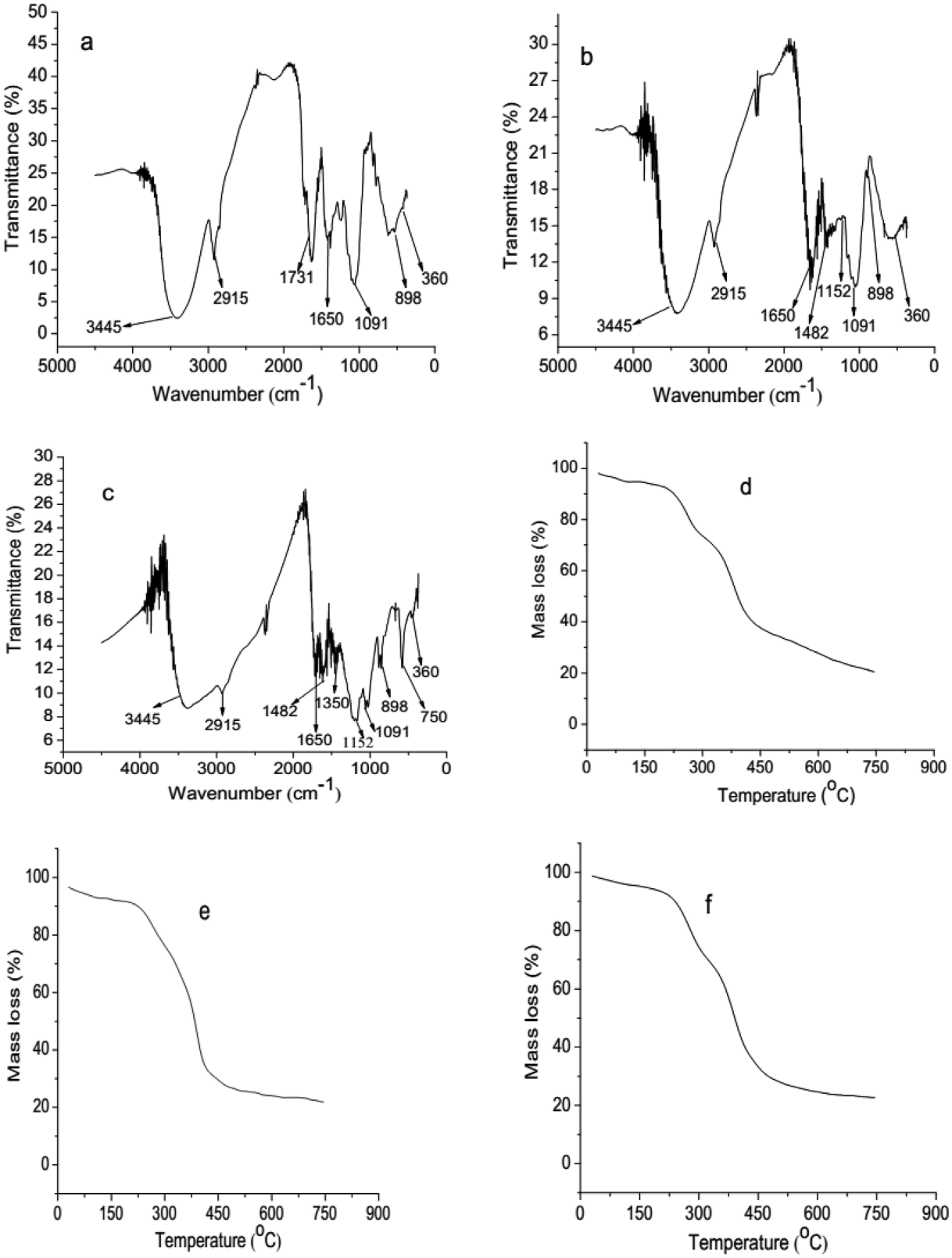

Fig. 1. FTIR of KS (a), KSC (b), KSS (c) and TG analysis of KS (d), KSC (e), KSS (f).

fraction was mixed with 1.6 mL of Tris-KCl buffer to which 0.5 mL of 30% trichloroacetic acid was added. 0.5 mL of 0.75% thiobarbituric acid was added and placed in a water bath for 45 min at 80 °C. This was then cooled in ice and centrifuged at 3000 g. The clear supernatant was collected and absorbance measured against a reference blank of distilled water at 532 nm. Lipid peroxidation in mg of MDA formed/mg protein was computed with a molar extinction coefficient of $1.56 \times 10^{-5}\,M^{-1}\,cm^{-1}$.

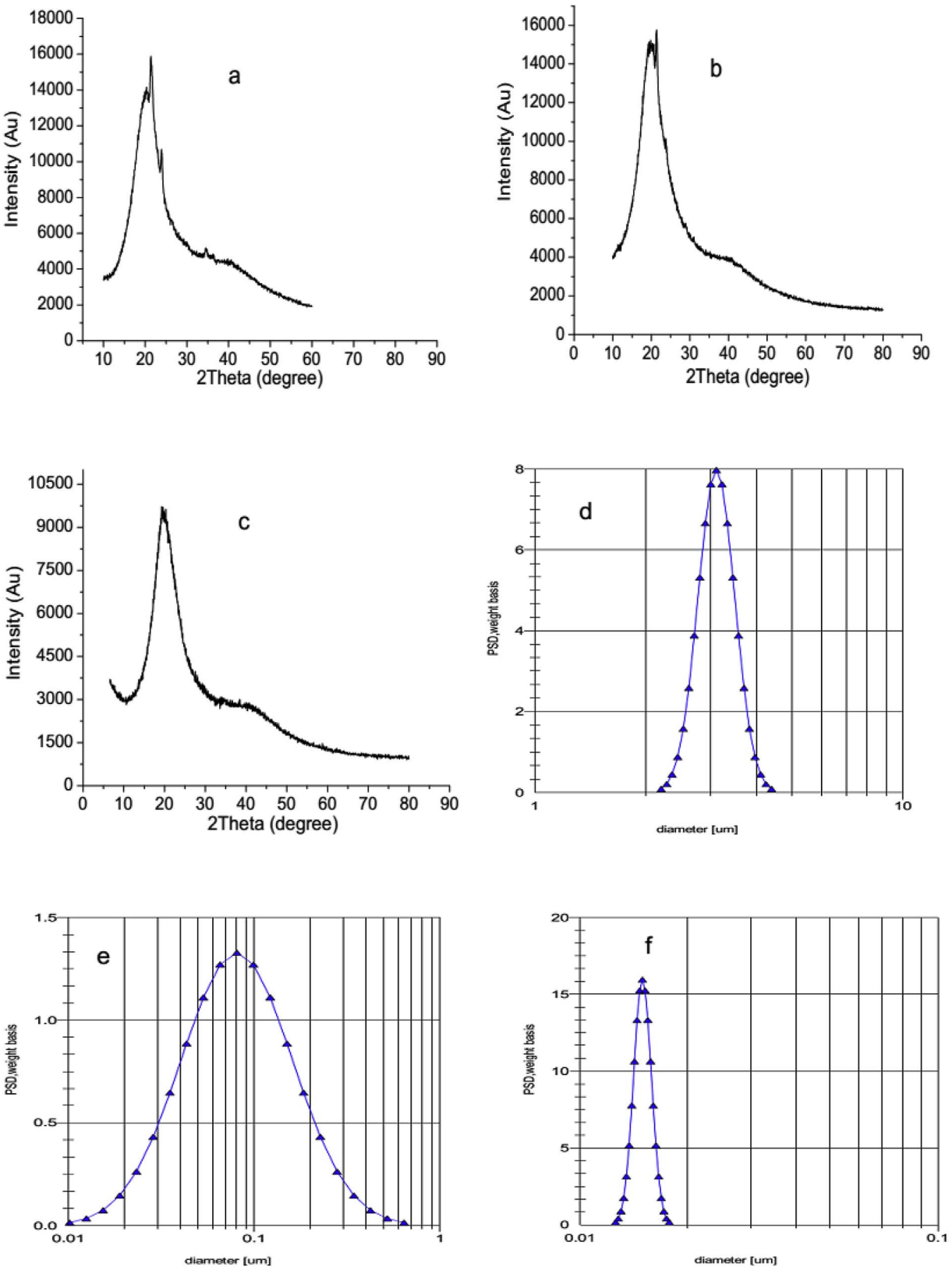

Fig. 2. XRD of KS (a), KSC (b), KSS (c) and PSD of KS (d), KSC (e), KSS (f).

2.9.9. Determination of nitric oxide

Serum/tissue nitrite (NO_2) and nitrate (NO_3^-) were estimated as index of nitric oxide (NO) production. Quantitation was based on the Greiss reaction according to the method of Bryan and Grisham [34].

2.9.10. Determination of myeloperoxidase activity

Myeloperoxidase (MPO) activity, an indicator of polymorphonuclear leukocyte accumulation, was assessed by measuring the H_2O_2-dependent oxidation of o-dianisidine according to the method of Bradley et al. [35].

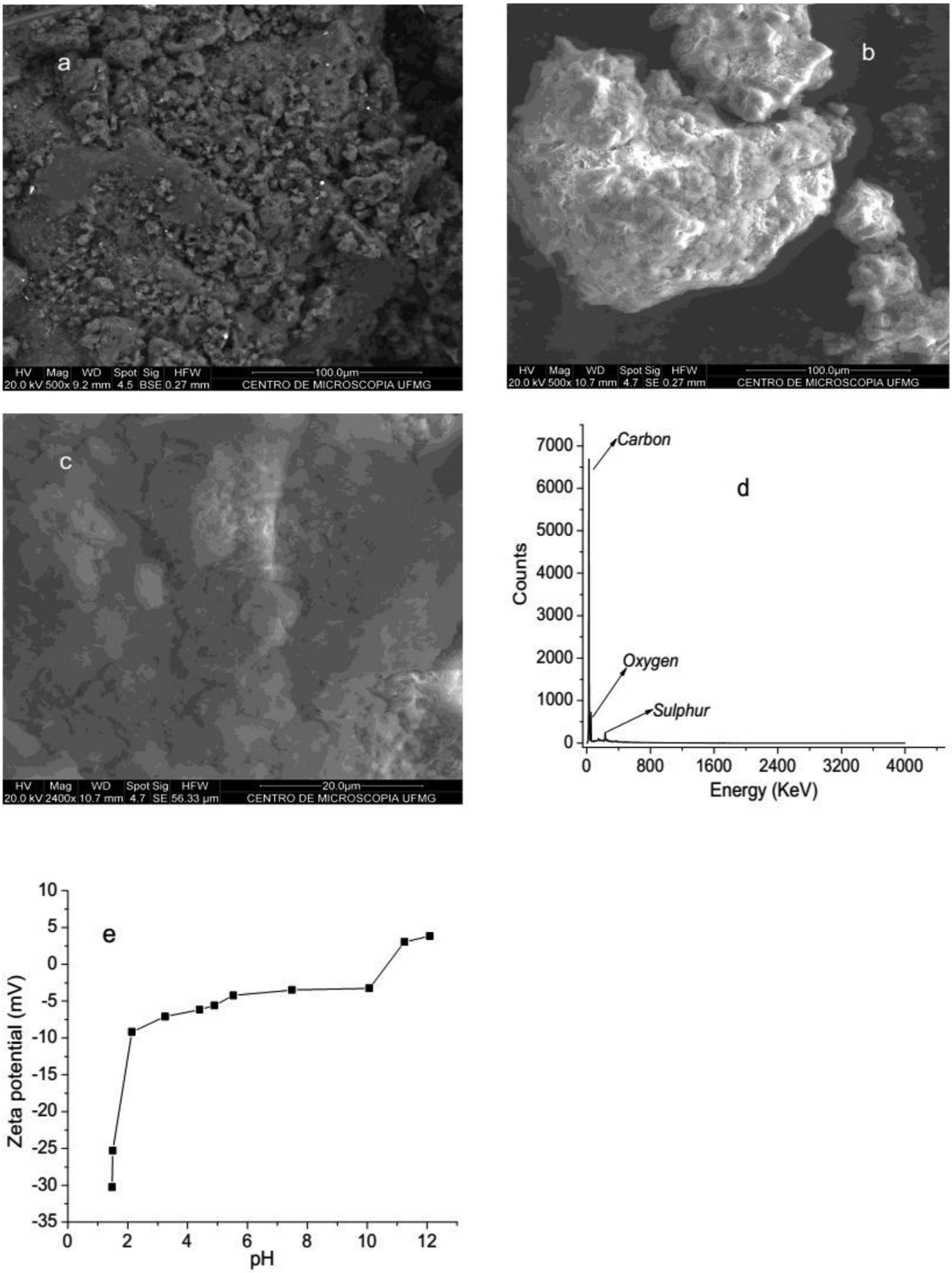

Fig. 3. SEM of KS (a), KSC (b), KSS (c), EDX of KSS (d) and zeta potential of KSS (e).

2.9.11. Protein assay

The protein concentrations in the homogenate samples were determined by means of biuret method as described by Gornall et al. [36] with some modifications. Potassium iodide was added to the reagent in other to prevent precipitation of Cu^{2+} ions as cuprous oxide.

2.10. Histopathology

For the histopathology examination, kidney tissues obtained from all experimental groups were fixed in 10% formaldehyde, dehydrated in graded alcohol and embedded in paraffin. The tissues were

Table 1
The kidney weight to body weight ratio of rats treated with KSS.

Treatment group	Body weight(g)	OSI (%)
Control	190.60 ± 34.77	0.63
50 mg/kg	182.30 ± 28.46	0.65
75 mg/kg	195.70 ± 31.14	0.62
100 mg/kg	187.20 ± 7.41	0.62

Data expressed as mean ± SD for five rats per group. OSI = organosomatic index.

subsequently cut into 4–5 mm sections by a microtome, fixed on the slides and stained with hematoxylin and eosin for light microscopic analyses.

2.11. Immunohistochemical assessment

Kidney specimens were fixed in neutral formalin solution (10%) and embedded in paraffin wax before being sectioned (thickness, 5 μm). Paraffin sections were deparaffinized in xylene, hydrated, and then placed in phosphate buffered saline (PBS; pH 7.6). Antigen retrieval was performed by boiling for 15 min in citrate buffer (0.01 M). Sections were treated with 3% hydrogen peroxide for 15 min to quench endogenous peroxidase activity, rinsed with deionized water, and then washed with PBS. Sections on the slides were treated with 130 μL of diluted biotinylated secondary antibody and incubated in a humidified chamber at room temperature for 30 min. After another wash, sections were incubated with diluted biotinylated secondary antibody at 23 °C in a moist chamber for 1 h. Detection of the antibody was performed using a Streptavidin–Horse Radish Peroxidase detection system with Diaminobenzidine (DAB) as the chromogen. Sections were counterstained with Mayer's hematoxylin, dehydrated, and then cover-slipped with Permount. Immunolabeling intensity was graded independently by two observers blinded to the experimental conditions on a scale modified from a previously described labeling [37], viz: Absence of messengial, tubular or matrix cells (−), presence of any one of messengial, tubular or matrix cells (+), presence of any two of messengial, tubular or matrix cells (++) and presence of all three of messengial, tubular and matrix cells (+++).

2.12. Statistical analyses

All data were expressed as mean ± standard error of the mean. Differences between the groups were determined by one-way analysis of variance (ANOVA) and *post hoc* testing was performed using Dunnet's multiple comparison tests (Graph Pad Prism software, Inc., San Diego, CA). Values were regarded as significantly different at $p < .05$.

3. Results

3.1. Characterization, water holding capacity and heavy metal adsorption capacity

The FTIR spectra of KS, KSC and KSS are presented in Fig. 1a, b and c; respectively. The spectra revealed bands corresponding to the isolation of KSC from KS and also the conversion of KSC to KSS. The decomposition pattern of KS, KSC and KSS is presented in Fig. 1d, e and f. The graph revealed loss in mass between 50 and 150 °C in KS, KSC and KSS. Both KS and KSS showed four different stages of mass loss while KSC showed three different stages of mass loss.

The X-ray diffractograms are shown in Fig. 2a, b and c. The crystallinity index (I_c) of KSC and KSS were determined using the height of 200 peak (I_{002}, $2\theta = 21.35°$) and the minimum intensity between the 200 and 110 peaks (I_{AM}, $2\theta = 17.25°$) which can be expressed as:

$$I_c(\%) = \left(\frac{I_{002} - I_{AM}}{I_{002}}\right) \times 100 \quad (4)$$

where I_{002} represents both crystalline and amorphous material while I_{AM} represents the amorphous material only. The diffraction pattern showed that KSC is of cellulose I which is characterized by low diffracted intensity at a 2θ value of around 17.25° [38]. The crystallinity of KSC was found to be 34.84% while that of KSS was 70.40%. The PSD of KS, KSC and KSS were found to be monomodal with mean distribution size of 0.0149 μm in KSS as presented in Fig. 2d, e and f.

The surface morphology of KS, KSC and KSS was examined using SEM, the micrograph is shown in Fig. 3a, b and c. The EDX and zeta potential results are also shown in Fig. 3d and e; respectively. The EDX result confirms the presence of sulphur on the surface of KSS indicating the formation of the sulphonate groups on KSS. The zeta potential of KSS increased with increase in pH. The suspension of KSS is considered stable since the absolute value of zeta potential is lower than −25 mV. The water holding capacity of KSS was found to be 6.30 g/g while the heavy metal adsorption capacity was found to be 19.913 mg/g towards Pb^{2+} and 19.677 mg/g towards Cu^{2+} ions.

3.2. Effect on renal somatic index

All the animals appeared clinically normal at the beginning and throughout the feeding. Table 1 summarizes the body weight for the treated and control group.

3.3. Renal function parameters

The results of the renal functional indices of rats fed with KSS are shown in Table 2. There were no significant changes in AST activity; except for a slight increase in the group administered with 50 mg/kg KSS. Likewise, exposure of rats to KSS at various doses did not elicit any

Table 2
Plasma clinical parameters in rats following 14 days treatment with KSS.

Parameters	Control	50 mg/kg	75 mg/kg	100 mg/kg
ALT, U/l	38.32 ± 4.01	43.48 ± 4.03	43.36 ± 4.05	37.35 ± 4.55
AST, U/l	43.39 ± 5.83	54.78 ± 2.68	45.78 ± 8.49	43.67 ± 2.94
Total Protein, g/dl	30.25 ± 1.02	33.86 ± 2.33	30.97 ± 1.99	30.34 ± 1.28
Albumin, g/dl	14.72 ± 2.75	12.73 ± 3.22	13.25 ± 2.60	14.39 ± 2.69
Globulin, g/dl	16.59 ± 2.15	22.52 ± 0.94	15.82 ± 4.59	14.79 ± 1.65
Albumin: Globulin ratio	0.88	0.56	0.84	0.97
Creatinine, μmol/l	80.77 ± 15.93	104.30 ± 15.64	85.32 ± 4.77	74.86 ± 0.84
Uric acid, mmol/l	0.45 ± 0.04	0.43 ± 0.06	0.51 ± 0.03	0.48 ± 0.02
Calcium, mmol/l	0.69 ± 0.26	0.17 ± 0.09*	0.51 ± 0.03	0.57 ± 0.12
Potassium, mEq/l	43.12 ± 7.54	14.02 ± 2.84*	11.28 ± 4.41*	33.25 ± 9.06
Sodium, mEq/l	0.02 ± 0.002	0.09 ± 0.004*	0.03 ± 0.006	0.04 ± 0.006*

Values are expressed as mean ± SD for five rats in each group. *Significantly different from control ($p < 0.01$).

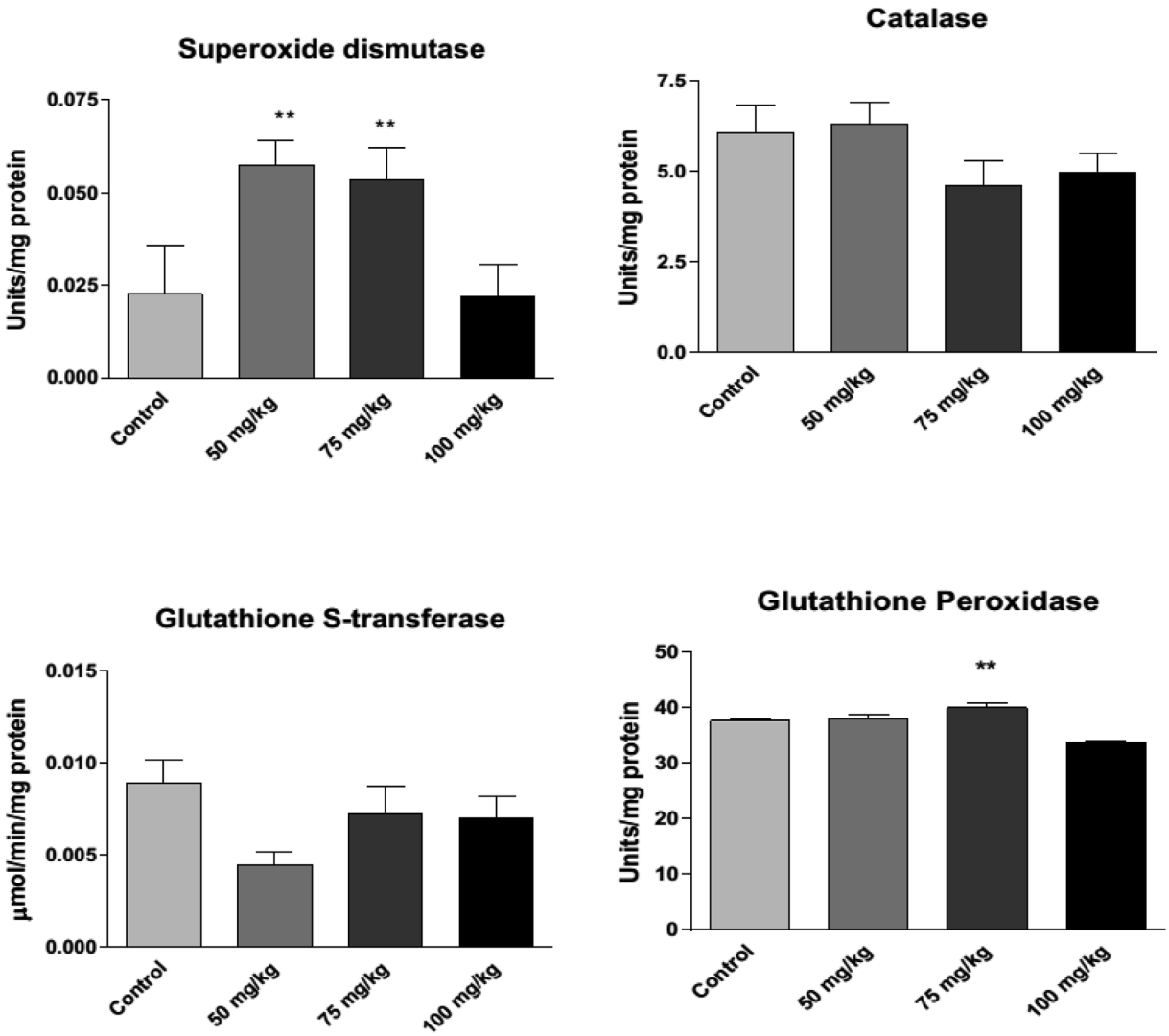

Fig. 4. Activities of SOD, CAT, GST and GPx in the kidney of rats treated with KSS for 14 consecutive days. Values are means ± SD of 5 animals per group. **p < 0.01 versus control.

changes in the total protein and albumin levels. The globulin levels of the treated groups were found within the range of the control group (16.59 ± 2.15 g/dl) except for rats exposed to 50 mg/kg KSS (22.52 ± 0.94 g/dl), although this was not significant when compared with the control group. Consequently, the Albumin: Globulin ratio was lower in the 50 mg/kg group (0.56) than in the control (0.88). Furthermore, the creatinine and uric acid levels were not significantly different across all treatment groups. However, there was a significant decrease in calcium and potassium ions levels in the 50 mg/kg KSS group when compared with the control. Contrariwise, there was a significant and dose-dependent increase in sodium ion levels in the treatment groups when compared with the control.

3.4. Tissue biochemical indices

Values obtained for SOD, CAT, GST and GPx are shown in Fig. 4. There was no significant change among the values obtained for CAT and GST when comparing the treated groups and the control but in the case of SOD and GPx, there was significant increase in their activities of rats exposed to 50 mg/kg KSS and 75 mg/kg KSS when compared with the control group. Fig. 5 presents the result of MDA, hydrogen peroxide and GSH levels. There were no significant changes in the MDA and hydrogen peroxide levels of rats exposed to KSS. However, the GSH levels were significantly depleted in rats treated with 100 mg/kg KSS. The level of NO and myeloperoxidase activity are also shown in Fig. 5. While exposure to KSS at different doses did not alter the NO level when compared with the control, the MPO activity was significantly reduced across all treatment groups.

3.5. Histopathology

The kidneys of control rats appear normal with no visible lesion. However, treatment with KSS (50 mg/kg) caused moderate cortical congestion. In addition, there were severe interstitial haemorrhage and presentation of protein casts in the tubules of rats exposed to KSS (75 and 100 mg/kg) as presented in Fig. 6.

3.6. Immunohistochemistry

COX-2, iNOS, Bcl-2 and p53 proetins were visualized by immunohistochemical staining of kidney tissue cross-sections in the KSS and control groups (Fig. 7). Immunolabeling intensity was graded independently by two observers blinded to the experimental conditions as shown in Table 3. The immune reactivity of COX-2 and iNOS were more intense in the kidney tissues of rats treated with KSS compared with respective controls. However, the immunnolabelling intensity of Bcl-2 and p53 showed similar pattern across all treatment groups.

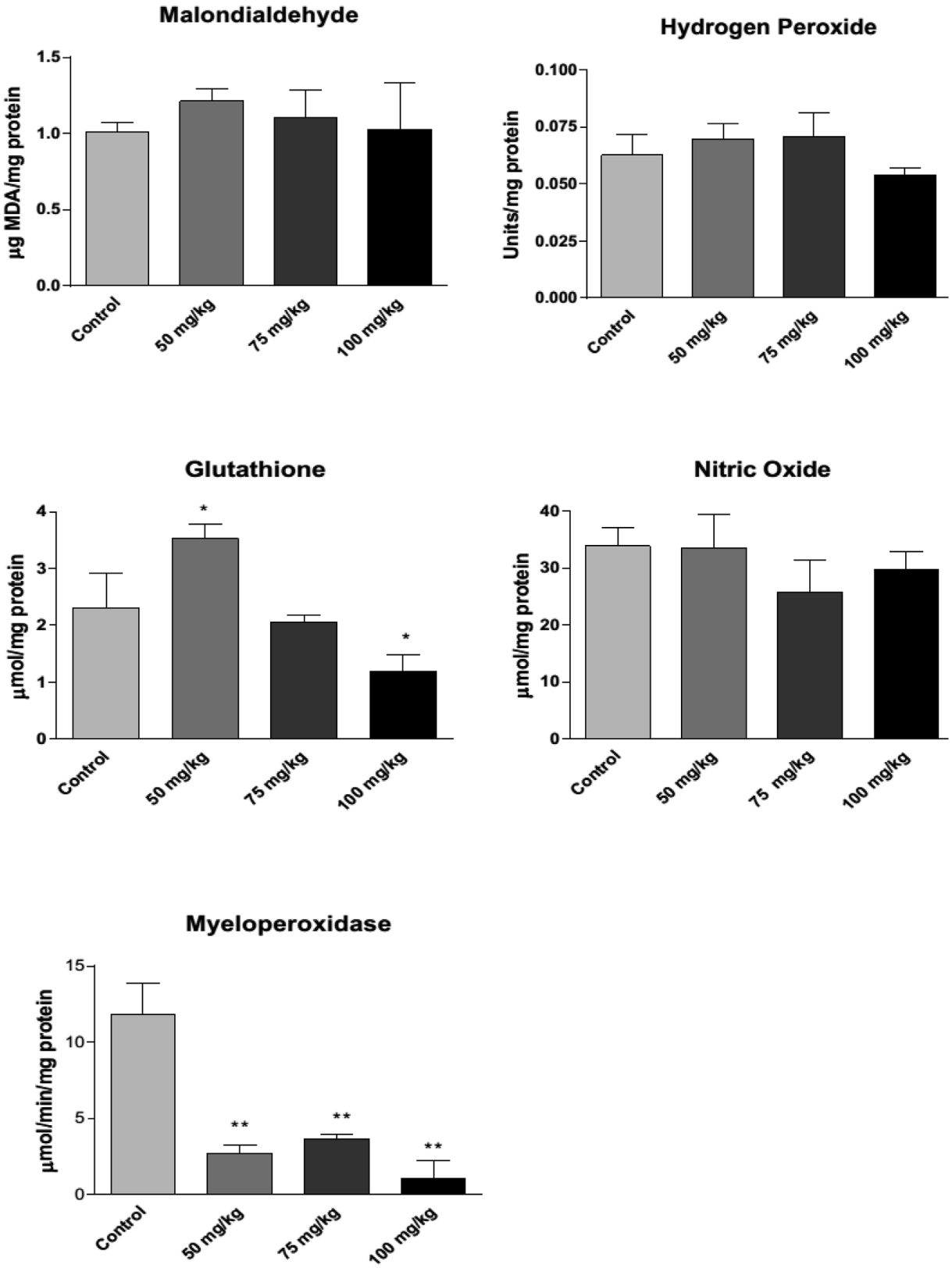

Fig. 5. Levels of MDA, H_2O_2 and GSH in the kidney of rats treated with KSS for 14 consecutive days (Values are means ± SD of 5 animals per group. *p < 0.05 versus control) and levels of NO and MPO in the kidney of rats treated with KSS for 14 consecutive days (Values are means ± SD of 5 animals per group. **p < 0.01 versus control).

4. Discussion

FTIR analysis was carried out to determine the different functional groups present in KS, KSC and KSS. The band corresponding to the amorphous characteristics of the cellulosic materials appeared at around 360 cm^{-1} in KS, KSC and KSS as previously reported [39] while peak corresponding to the C-O-C stretching of the β-1,4-glycosidic linkages of the glucopyranose units of the cellulose appeared at 898 cm^{-1}.

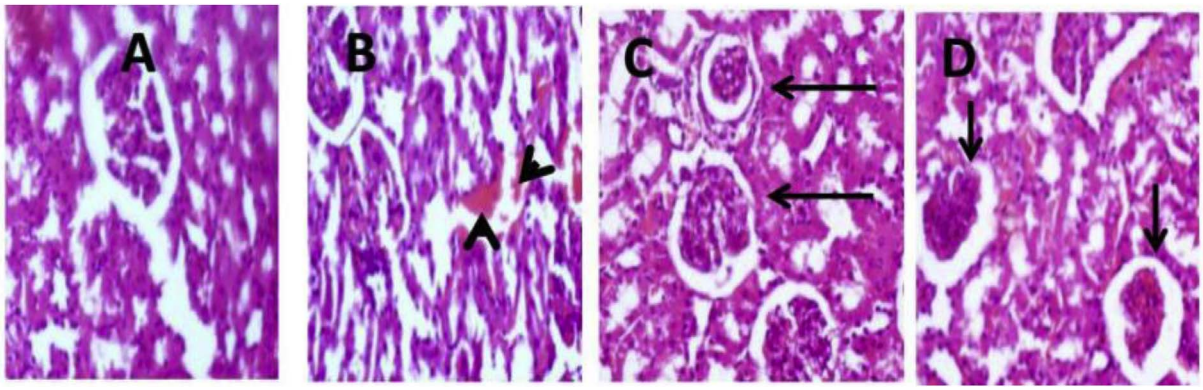

Fig. 6. Representative photomicrograph of hematoxylin and eosin-stained sections of kidney from the experimental groups. The kidneys of control rats appear normal but there are protein casts in some tubular lumen (arrow) and cortical mild congestion (arrow head) in renal morphology of rats exposed to KSS. (A) Control (B) 50 mg/kg KSS; (C) 75 mg/kg KSS and (D) 100 mg/kg KSS. Original magnification: X 400.

The spectra also revealed bands at 1482 cm^{-1} and 1340 cm^{-1} which were assigned to the vibrational frequencies of H-C-H bending and H-O-C bending, respectively while peaks at 1091 and 1152 cm^{-1} were attributed to the deformation of the C-H rocking vibration and the C-O-C pyranose ring skeleton. The peak at 2915 cm^{-1} suggests the C-H stretching of CH_2 in all the spectra. The peak at 3445 cm^{-1} was common to all the spectra which may be attributed to the presence of OH functional group in them. The bands at around 750 cm^{-1} and 1350 cm^{-1} indicates the presence of sulphonate group in KSS [40].

The loss in mass between 50 and 150 °C in KS, KSC and KSS as shown in the TG graph may be attributed to loss of volatile molecules and internally bound water molecules in the samples. Thermal degradation of cellulose and cellulose containing materials have been reported to release combustible volatile compounds such as

Table 3
The grading of intensity of immunostaining.

	Control	50 mg/kg	75 mg/kg	100 mg/kg
COX-2	+	+ +	+ +	+ +
iNOS	+ +	+ + +	+ + +	+ +
BCl-2	+ +	+ +	+ +	+ +
p53	+ +	+ +	+ + +	+ +

A: Control; B: 50 mg/kg KSS; C: 75 mg/kg KSS; D: 100 mg/kg KSS; KSS: Sulphonated nanocellulose from *Khaya sengalensis*; +: presence of any one of messengial, tubular or matrix cell; + +: presence of any two of messengial, tubular or matrix cells; + + +: presence of all three of messengial, tubular and matrix cells.

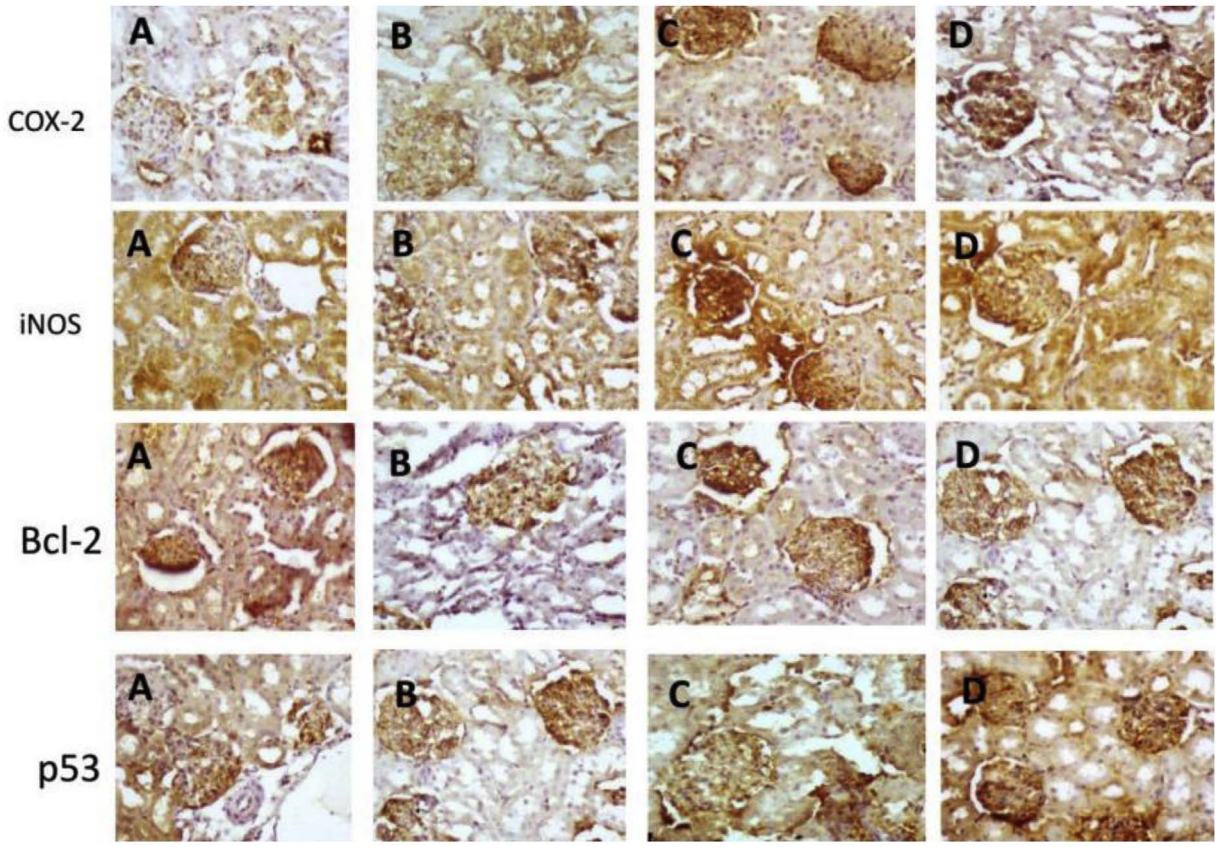

Fig. 7. Photomicrographs of immunohistochemically stained sections to detect COX-2, iNOS, Bcl-2 and p53 in rats treated with KSS. (A) Control; (B) 50 mg/kg KSS; (C) 75 mg/kg KSS and (D) 100 mg/kg KSS. Original magnification: X 400.

butanedione, methanol, acetaldehyde, acetic acid and propenal [41], these compounds may have also been released during this temperature range (50–150 °C). Loss in mass observed at around 165–240 °C in KSC and KSS was considered as being due to degradation leading to 1,4 and 1,6 anhydroglucopyranoside. Similar observation at 165–240 °C in KS was considered to be due to loss of hemicellulose and some other volatile matters while loss at around 240–430 °C was attributed to loss of lignocelluloses. Degradation at 351 °C was attributed to depolymerization at 1,4 glycosidic bond while loss found at temperatures above 450 °C was taken to be due to loss of lignin and char.

The diffractograms showed increase in crystallinity from KSC to KSS which may be due to the removal of most of the amorphous regions in KSC. This has shown that the crystallinity of KSS exceeds its amorphous form and that the crystallinity is within the range of most crystalline materials [42]. The SEM micrograph revealed the surface of KS to be heterogeneous which suggests the presence of different functional groups at the surface since this is a raw plant seed. The surface also looks rough with some pits. The surface of KSC looks homogeneous with white gel appearance which might be due to the removal of hemicellulose, lignin and other functional groups present in the starting material (KS). Moreover, surface of cellulose contains mainly the hydroxyl group so the surface is expected to be homogeneous. The micrograph of KSS reveals a flaky surface with agglomerations at the surface.

The water holding capacity of KSS was found to be 6.30 g/g. This value is an expression of the ability of KSS to hold water; this parameter plays an important role in understanding the release mechanism of plant drug in biological system most especially in encapsulated drugs. This value is lower than value reported by Zain et al. [42] for *Citrus grandis* (12.75 g/g), grapefruit (9.77 g/g) and orange (11 g/g). The heavy metal adsorption capacity of KSS was found to be 19.913 mg/g towards Pb^{2+} and 19.677 mg/g towards Cu^{2+} ions. These metals have been associated with hepatotoxicity and are toxic when they get into human system [43]. This is an indication that KSS may be used to adsorb these poisonous metals from systems where they are not required such as in biological system.

The rat body weights across all treatment groups were not significantly changed, indicating that the doses administered had no significant effect on the organosomatic index, which may be due to the non-fatty nature of KSS or the ability of the kidney to excrete it over the studied period of time. Although reduction in albumin may be referred to as part of nephrotic syndrome in which protein is lost in the urine due to kidney damage [44] but in this present study, the observed reduction in albumin level had no significant effect when compared with the control group suggesting an adaptative response of the tissue to metabolic changes [45]. Albumin: Globulin ratio plays key role as an index in understanding health conditions. In rats treated with 100 mg/kg KSS, the ratio value was higher than the control whereas, the ratio value was lower in the 50 mg/kg group in comparison with the control. Similar observation had been reported by Olorunnisola et al. [46] using *T. violacea* rhizomes extract on high cholesterol diet fed rats. Creatinine level is an important indicator of renal health or function. The recorded high creatinine value in rats administered 50 mg/kg KSS may not necessarily represent true glomerular filtration rate but may be due to increase in creatinine production as a result of intense acrobatic movement of the rats within this group which could have resulted in increased muscle breakdown thus increase in creatinine production. However, there was no significant difference between the values obtained for the treated groups and the control. The reduction in serum uric acid may suggest the ability of KSS to reduce uric acid at the administered concentration (50 mg/kg body weight). This observation agrees with the postulated mechanism of action of methotrexate previously reported by Lee et al. [47]. Just as the carboxyl and amine groups in methotrexate may be responsible for its activity, the sulphonate group in KSS may also be responsible for this activity; although this mechanism requires further validation. This also shows the potential of KSS to promote the excretion of uric acid from the blood into urine. At increased doses of KSS (75 and 100 mg/kg), the uric acid level also increased. This finding is in agreement with previously published work [48]. This may be due to the inability of the kidney to eliminate uric acid efficiently as a result of the high amount of KSS administered in these studied groups. Uric acid can serve as an antioxidant within extracellular conditions but when it enters the cell, it can cause oxidative stress which suggests that KSS may have induced oxidative stress at high concentration. Although there are compelling reasons to consider uric acid as a false risk factor for kidney disease since uric acid is primarily excreted by the kidney but care needs to be taken to avoid unnecessary rise in its level.

The supposed hypocalcaemia and hypokalemia observed in this study might be due to failure in renal function or hypoparathyroidism. The intake of KSS may have distorted the calcium/potassium balance. It is plausible that the sulphonate group in KSS may have formed a bond with calcium and potassium ions in the fluid of the rats leading to a reduction in the available electrolytes. Apart from these, KSS increased sodium ions level in the rats. Typically, hypernatremia could occur when there is a primary dehydration with loss of water without electrolyte loss. This disruption of the electrolyte balance may also be due to the electronic interaction between the sulphonate group in KSS and the electrolytes, and could represent one of the mechanisms of KSS-induced renal toxicity. Our data corroborate the report of Gil et al. [49], who showed that orally administered casein nanoparticles elevated sodium ion level in rats.

Normal kidney function is protected from oxidative stress by the antioxidant defense system comprising of SOD, CAT, GPx, GST, and GSH. The basic biochemistry of antioxidant enzymes involves the rapid dismutation of superoxide anion to H_2O_2 by SOD thereby preventing the former from participating in the Haber Weiss reaction to produce the highly pernicious hydroxyl radicals. Moreover, the cell is further protected from the oxidizing action of H_2O_2 by its subsequent conversion to water and oxygen by CAT or GPx. The present investigation showed that while administration of KSS mediated an increase in SOD and GPx activities, it insignificantly decreased the activities of CAT and GST in the kidney of rats. The increase in the activities of these SOD and GPx indicate their inductive and adaptive responses in KSS-treated rats.

Glutathione, a non-enzymatic antioxidant, is widely involved in oxido-reduction reactions in the presence of GPx that oxidizes GSH to GSSG. The increase in GSH level was significant only at the 50 mg/kg dose, in KSS-treated rats. The increase in GSH observed in KSS-treated rats could protect the tissues against oxidative stress by scavenging hydroxyl radicals and singlet oxygen directly, detoxifying H_2O_2 and lipid peroxides by the catalytic actions of GST and GPx [50]. This could have contributed to the observed normalcy in MDA and H_2O_2 levels in comparison with control groups. However, at the highest dose of 100 mg/kg KSS, there was a marked depletion of GSH levels, indicating the potential for renal oxidative stress.

Recent study [51] has shown that reduced level of NO may be associated with improvement of chronic pain. Although increased level of NO is beneficial due to its role in cellular activities but KSS may be considered not to have significant effect on the NO level in the treated groups. Myeloperoxidase plays a role in atherosclerosis due to its involvement in inflammation. It has been considered as an independent risk-factor for coronary artery diseases. Previous study has also shown a correlation between coronary artery disease and rise in myeloperoxidase level [52]. The release of myeloperoxidase has been reported to be promoted by increased neutrophils [53] indicating that the low level of myeloperoxidase in the treated groups might be suggestive of the potential of KSS being able to play intervention role in coronary dysfunction and oxidative stress. Interestingly, we observed increased immunohistochemical expressions of COX-2 and iNOS in the kidney of KSS-treated rats, prompting us to propose that KSS has the potential to induce inflammation at the tested doses. In order to find out if inflammation induced by KSS was linked with apoptosis, we carried out

the immunohistochemical expressions of Bcl-2 and p53. This is because apoptosis is recognized as an early indicator of toxicity [54]. The tumour suppressor protein p53 is a stress-responsive protein and it plays a critical role in regulating both cell survival and death depending on the cell type and nature of stress involved [54]. There were no significant changes in the expressions of these apoptotic proteins indicating KSS-induced inflammation was not linked to the mitochondrial apoptotic pathway. However, molecular studies are needed to reveal a link with the receptor-mediated pathway.

Conflicts of interest

The authors declare that there are no conflicts of interests.

Acknowledgements

This research was partly supported by TWAS-CNPq. The authors are also grateful to TWAS-CNPq for awarding a postdoctoral fellowship at Universidade Federal de Minas Gerais, Minas Gerais, Brazil.

Transparency document

Transparency document related to this article can be found online at http://dx.doi.org/10.1016/j.cbi.2018.02.015.

References

[1] H.S. Abou Seif, Physiological changes due to hepatotoxicity and the protective role of some medicinal plants, Review article; Beni-suef, Uni. J. Basic Appl. Sci. 5 (2016) 134–146.
[2] M. Ekor, O. Adeyemi, C.A. Otuechere, Management of anxiety and sleep disorders: role of complementary and alternative medicine and challenges of integration with conventional orthodox care, Chin. J. Intergr. Med 199 (2013) 5–14.
[3] S.K. Xavier, S.M. Haneefa, D.R. Anand, P.R. Polo, R. Maheshwari, C.S. Shreedhara, M.M. Setty, Antioxidant and nephroprotective activities of the extract and fractions of *Homonoia riparia* Lour, Pharmacogn. Mag 13 (2017) 25–30.
[4] K. Sulakhiya, V.K. Patel, R. Saxena, J. Dashore, A.K. Srivastava, M. Rathore, Effect of *Beta vulgaris* Linn leaves extract on anxiety and depressive-like behavior and oxidative stress in mice after acute restraint stress, Phcog. Res. 8 (2016) 1–7.
[5] O.F. Kunle, H.O. Egharevba, P.O. Ahmadu, Standardization of herbal medicines - a review, Int. J. Biodvers. Conserv 4 (2012) 101–112.
[6] F. Stickel, D. Schuppan, Herbal medicine in the treatment of liver diseases, Dig. Liver Dis. 39 (2007) 293–304.
[7] J.D. Imig, M.J. Ryan, Immune and inflammatory role in renal disease, Compr. Physiol 3 (2013) 957–976.
[8] K.K. Wong, S.O. Cheung, L. Huang, J. Niu, C. Tao, C.M. Ho, C.M. Che, P.K. Tam, Further evidence of the anti-inflammatory effects of silver nanoparticles, Chem. Med. Chem. 4 (2009) 1129–1135.
[9] A. Dufresne, Nanocellulose: a new ageless bionanomaterial, Mater. Today 16 (2013) 220–227.
[10] E. Lam, K.B. Male, J.H. Chong, A.C.W. Leung, J.H.T. Luong, Applications of functionalized and nanoparticle-modified nanocrystalline cellulose, Trends Biotechnol. 30 (2012) 283–290.
[11] L.S. Pachuau, A mini review on plant-based nanocellulose: production, sources, modifications and its potential in drug delivery applications, Mini Rev. Med. Chem. 15 (2015) 543–552.
[12] M. Roman, Toxicity of cellulose nanocrystals, A review, Ind. Biotechnol. 11 (2015) 25–33.
[13] B.J. Harper, A. Clendaniel, F. Sinche, D. Way, M. Hughes, J. Schardt, J. Simonsen, A.B. Stefaniak, S.L. Harper, Impacts of chemical modification on the toxicity of diverse nanocellulose materials to developing zebrafish, Cellulose 23 (2016) 1763–1775.
[14] A. Muller, F. Wesarg, N. Hessler, F.A. Muller, D. Kralisch, D. Fischer, Loading of bacterial nanocellulose hydrogels with proteins using a high-speed technique, Carbohydr. Polym. 106 (2014) 410–413.
[15] F.V. Pereira, E.L. de Paula, J.P. de Mesquita, D.D. Lucas, V. Mano, Bio-based nanocomposites obtained by incorporation of cellulose nanocrystals into biodegradable polymers through casting, layer-by-layer or electrospinning methods, Quím. Nova 37 (2014) 1209–1219.
[16] J. Trifol, D. Plackett, C. Sillard, O. Hassager, A.E. Daugaard, J. Bras, P. Szabo, A comparison of partially acetylated nanocellulose, nanocrystalline cellulose, and nanoclay as fillers for high-performance polylactide nanocomposites, J. Appl. Polym. Sci. 133 (2016) 43257.
[17] L. Brinchi, F. Cotana, E. Fortunati, J. Kenny, Production of nanocrystalline cellulose from lignocellulosic biomass: technology and applications, Carbohydr. Polym. 94 (2013) 154–169.
[18] N.A. Beinborn, R.O. Williams, Polymeric biomaterials in pulmonary drug delivery. Polymeric biomaterials, medicinal and pharmaceutical applications; Volume 2, CRC press, Taylor and Francis group; Broken sound parkway NW, Boca Raton, Florida, USA, 2013, pp. 563.
[19] A. Adewuyi, R.A. Oderinde, B.V.S.K. Rao, R.B.N. Prasad, Chemical composition and molecular speciation of the triacylglycerol of the oils of *Lonchocarpus sericeus* and *Lonchocarpus cyanescens*, Nat. Prod. Res. 26 (2012) 1954–1956.
[20] A. Adewuyi, F.V. Pereira, Cellulose nanocrystals from underutilized *Polythia longifolia* seed, Periodico Tche Quim 14 (2017) 10–18.
[21] M. Zhang, C.J. Zhang, S. Shrestha, Study on the preparation technology of superfine ground powder of Agrocybe chaxingu Huang, J. Food Eng. 67 (2005) 333–337.
[22] A. Adewuyi, C.A. Otuechere, Z.O. Oteglolade, E.I. Unuabonah, Evaluation of the safety profile and antioxidant activity of fatty hydroxamic acid from underutilized seed oil of *Cyperus esculentus*, J. Acute Dis 4 (2015) 230–235.
[23] S. Merkle, W. Hanke, Long-term starvation in Xenopus laevis Daudin-II. Effects on several organs, Comp. Biochem. Physiol. A Comp. Physiol. 90 (1988) 491–495.
[24] C.A. Otuechere, O. Adesanya, P. Otsupius, N. Seyitan, Alterations in morphology and hepatorenal indices in rats subacutely exposed to bitumen extract, Ren. Fail. 38 (2016) 1545–1553.
[25] R.D. Wijesekera, G.K.H. de Alwis, D. Vithana, W.D. Ratnasooriya, Serum levels of some electrolytes of captive Sri Lankan elephants, Gajah 29 (2008) 24–27.
[26] K.V. Pramina, P.T. Mincy, P.A. Joseph, V. Lisha, K.A. Mercy, V. Ramnath, Levels of calcium, sodium and potassium in plasma as influenced by anticoagulants, J. Vet. Anim. Sci. 44 (2013) 72–75.
[27] H.P. Misra, I. Fridovich, The univalent reduction of oxygen by reduced flavins and quinines, J. Bio. Chem. 247 (1972) 188–192.
[28] H. Luck, Catalase, in: J. Bergmeyer, M. Grabi (Eds.), Methodsof Enzymatic Analysis,Vol.II, Academic Press, New York, 1974, pp. 885–890.
[29] J.T. Rotruck, A.L. Pope, H.E. Ganther, A.B. Swanson, D.G. Hafeman, W.G. Hoekstra., Selenium: biochemical role as a component of glutathione peroxidase, Science 179 (1973) 588–590.
[30] W.H. Habig, M.J. Pabst, W.B. Jacoby, Glutathione-S-transferases: the first enzymatic step in mercapturic acid formation, J. Biol. Chem. 249 (1974) 7130–7139.
[31] E. Beutler, O. Duron, B.M. Kelly, Improved method for the determination of blood glutathione, J. Lab. Clin. Med. 61 (1963) 882–888.
[32] S.P. Wolff, Ferrous ion oxidation in the presence of ferric ion indicator xylenol orange for measurement of hydroperoxides, Methods Enzymol. 233 (1994) 182–189.
[33] R. Varshney, R.K. Kale, Effect of calmodulin antagonist on radiation induced lipid peroxidation in microsomes, Int. J. Rad. Biol. 58 (1990) 733–743.
[34] N.S. Bryan, M.B. Grisham, Methods to detect nitric oxide and its metabolites in biological samples, Free Radic. Biol. Med. 43 (2007) 645–657.
[35] P.P. Bradley, D.A. Priebat, R.D. Christensen, C. Rothstein, Measurement of cutaneous inflammation: estimation of neutrophil content with an enzyme marker, J. Invest. Dermatol. 78 (1982) 206–209.
[36] A.G. Gornall, C.J. Bardawill, M.M. David, Determination of serum proteins by means of the biuret reaction, J. Biol. Chem. 177 (1948) 751–766.
[37] B. Baykara, I. Tekmen, S.C. Micili, C. Ozogul, Prophylactic and therapeutic effects of Carnosine in Ischemia reperfusion injury of liver, Turkiye Klinikleri J. Med. Sci. 30 (2010) 1896–1905.
[38] H. Lu, Y. Gui, L. Zheng, X. Liu, Morphological, crystalline, thermal and physico-chemical properties of cellulose nanocrystals obtained from sweet potato residue, Food Res. Int. 50 (2013) 121–128.
[39] C. Parida, S.K. Dash, C. Pradhan, FTIR and Raman studies of cellulose fibers of *Luffa cylindrical*, Open J. Comp. Mat 5 (2015) 5–10.
[40] G. Socrates, Infrared and Raman Characteristic Group Frequencies, John Wiley & Sons, New York, 2004, pp. 219–220.
[41] J.P.S. Morais, M.D. Rosa, M.D.M.D. Filho, L.D. Nascimentoa, D.M. do Nascimento, A.R. Cassales, Extraction and characterization of nanocellulose structures from raw cotton linter, Carbohydr. Polym. 91 (2013) 229–235.
[42] N.F.M. Zain, S.M. Yusop, I. Ahmad, Preparation and characterization of cellulose and nanocellulose from Pomelo (Citrus grandis) Albedo, J. Nutr. Food Sci. 5 (2014) 334.
[43] M. Rizwan, R. Yahya, A. Hassan, M. Yar, A.D. Azzahari, V. Selvanathan, F. Sonsudin, C.N. Abouloula, pH sensitive hydrogels in drug delivery: brief history, properties, swelling, and release mechanism, material selection and applications, Polymers 9 (2017) 137–174.
[44] A.M. Al-Attar, Vitamin E attenuates liver injury induced by exposure to lead, mercury, cadmium and copper in albino mice, Saudi J. Biol. Sci. 18 (2011) 395–401.
[45] M. Hübner, S. Mantziari, N. Demartines, F. Pralong, P. Coti-Bertrand, M. Schafer, Postoperative albumin drop is a marker for surgical stress and a predictor for clinical outcome: a pilot study, Gastroenterol. Res. Pract 2016 (2016) 8743187.
[46] S.O. Olorunnisola, G. Bradley, A.J. Afolayan, Protective effect of T. violacea Rhizome extract against hypercholesterolemia-induced oxidative stress in wistar rats, Mol 17 (2012) 6033–6045.
[47] J.J. Lee, V.P. Bykerk, G.K. Dresser, G. Boire, B. Haraoui, C. Hitchon, C. Thorne, D. Tin, S. Jamal, E.C. Keystone, J.E. Pope, Reduction in serum uric acid may be related to methotrexate efficacy in early rheumatoid arthritis: data from the Canadian early arthritis cohort (CATCH), Clin. Med. Insights Arthritis Musculoskelet. Disord 9 (2016) 37–43.
[48] P. Emery, F.C. Breedveld, E.M. Lemmel, J.P. Kaltwasser, P.T. Dawes, B. Gömör, F. Van Den Bosch, D. Nordström, O. Bjorneboe, R. Dahl, K. Horslev-Petersen, A. Rodriguez De La Serna, M. Molloy, M. Tikly, C. Oed, R. Rosenburg, I. Loew-Friedrich, A comparison of the efficacy and safety of leflunomide and methotrexate for the treatment of rheumatoid arthritis, Rheumatol 39 (2000) 655.
[49] A.G. Gil, J.M. Irache, I. Peñuelas, C.J. González, A. López, Toxicity and

biodistribution of orally administered casein nanoparticles, Food Chem. Toxicol. 106 (2017) 477–486.
[50] E.O. Farombi, I.A. Adedara, A.B. Oyenihi, E. Ekakitie, S. Kehinde, Hepatic, testicular and spermatozoa antioxidant status in rats chronically treated with Garcinia kolaseed, J. Ethnopharmacol. 146 (2013) 536–542.
[51] M.G. Rocha, V.A. Gomes, J.E. Tanus-Santos, J.C. Rosa-e-Silva, F.J. Candido-dos-Reis, A.A. Nogueira, O.B. Poli-Neto, Reduction of blood nitric oxide levels is associated with clinical improvement of the chronic pelvic pain related to endometriosis, Braz. J. Med. Biol. Res. 48 (2015) 363–369.
[52] F.A. Mayyas, M.I. Al-jarrah, K.S. Ibrahim, K.H. Alzoubi, Level and significance of plasma myeloperoxidase and the neutrophil to lymphocyte ratio in patients with coronary artery disease, Exp. Ther. Med 8 (2014) 1951–1957.
[53] L. Xing, B.F. Boyce, Regulation of apoptosis in osteoclasts and osteoblastic cells, Biochem. Biophys. Res. Commun. 328 (2005) 709–720.
[54] R. Nithipongvanitch, W. Ittarat, J.M. Velez, R. Zhao, D.K. St Clair, T.D. Oberley, Evidence for p53 as guardian of the cardiomyocyte mitochondrial genome following acute adriamycin treatment, J. Histochem. Cytochem. 55 (2007) 629–639.